Electronic Supplementary Material (ESI) for RSC Advances.

Supplementary information

Micellar $Zn(Cys)_2$ Complex Mimics the Chloroperoxidase Active Site

Mohammad M. Akbarzadeh[a*]

[a]School of Biological Sciences, Institute for Research in Fundamental Sciences, Tehran, Iran

CORRESPONDING AUTHOR FOOTNOTE

Email address: Akbarzadeh.ibb@ut.ac.ir (M. M. Akbarzadeh)

Tel.: +4917640503860; Fax: +98-2166404680

Materials and Methods

Materials

Chloroperoxidase (CPO), Dodecyltrimethylammonium bromide (DTAB), Sodium dodecyl sulfate (SDS) and L-Cys were obtained from Sigma, USA. H_2O_2, $MnCl_2$, $FeCl_3$, $CuCl_2$ and $ZnCl_2$ purchased from Merck, Germany. D_2O and DCl 99.9% provided from ARMAR Chemicals. Phosphate buffer 5 mM was prepared at pH levels of 3 and 7 and store at 4°C. Mixed micelle prepared by addition of 5 mM SDS to a solution of 25 mM DATB (1:5 SDS/DTAB molar ratio).

Methods

Kinetic analysis: UV-vis spectra recorded via a Shimadzu-3100 spectrophotometer. Steady-State kinetic of chlorination of thionine and NR monitored dechlorination of strong colored solution at 598 nm and 526 nm, respectively. Based on the method reported by Hager, chlorination of thionine substrate is measured via monitoring of the bleaching of the strong violet color at 598 nm (ε_{598}= 6.02×10^4 $M^{-1}. Cm^{-1}$) [1,2]. In case of neutral red (NR), chlorination contributes in decolorizations of substrate red color which monitors at 526 nm (ε_{526}= 1.6×10^4 $M^{-1}. Cm^{-1}$).

^1H NMR analysis performed with a Bruker Avance 300-MHz NMR spectrometer. SDS/DTAB (2 mM/8 mM) diluted in D_2O at a pH level of 3 (DCl used to reduce the pH of solution). $ZnCl_2$ (0.1 mM) injected to a solution of L-Cys (0.12 mM) at a pH level of 7 in order to create $Zn(Cys)_2$ complex.

Differentiate Scanning Calorimetry (DSC): Calorimetric plots of miellar solutions obtained via a Nano calorimeter (N DSCII, Calorimetric Scientific Corporation, Model 6100-Moskow-Russia). Denaturation of micellar scaffold, occurred via thermal titration (0-100 °C), contributes in thermal changes which is correspond to the non-covalent interactions and forces. $ZnCl_2$/L-Cys (0.4 mg/0.5

mg) was added to SDS/DTAB solution (5 mM/25 mM) at low pH levels. The reaction mixture loaded to cell in order to undergoes thermal titration.

Isothermal Titration Calorimetry (ITC) experiments were performed using a VP-ITC ultrasensitive titration calorimeter (Nano-Cal, LLC, Northampton, and MA). ITC involving a reference cell and a sample cell placed in an adiabatic shell isolate system. The reference cell was loaded with degassed aqueous solution of SDS/DTAB (5 mM/25 mM), and sample cell was loaded with Zn(II)/L-Cys prepared at pH level of 3. $ZnCl_2$/L-Cys (3 mM/4 mM) diluted in acetate buffer was injected by syringe into the sample cell. This process involved 30 injections, with 5 µl for the first injection fallowed by adding 10 µl for each subsequent sample. Each injection took 6 seconds which occurred totally at 3 minutes intervals. The heat generated from injection of $Zn(Cys)_2$ to the aqueous solution was subtracted to obtain the final curves that represents the insertion of Zn(II) complex inside micellar scaffold. The enthalpy changes due to the interaction of injected ligand into the sample cell measure at constant temperature 27 °C. A water bath controlled the temperature during the experiment.

Transition Electron Microscopy (TEM): TEM images were obtained from a ZEISS electron microscope (USA) operated at 100 kV.

Dynamic light Scattering (DLS): Dynamic radii and zeta potential of micellar scaffold obtained using DLS (Malvern Instruments, USA).

Results

Nucleic Magnetic Resonance (NMR) analysis: ^{1}H NMR analysis indicates that addition of L-Cys to a solution of Mn(II), Fe(III) and Cu(II) contributes to the formation of cystine, while Zn(II) creates a stable aromatic complex at a pH level of 7 (Fig. 1S). Then, Zn/L-Cys complex appears as a suitable active center for enzyme mimic. The novel achievements in this approach motivated by

the formation of $Zn(Cys)_2$ complex. Based on previous achievements, transition metals involving Mn, Fe and Cu are able to form thiol bonding at low pH levels [3,4]. L-Cys has the great potential for formation of cystine in the presence of strong oxidant like Fe(III) [3]. Thiol bond formation would deshielded the CH and CH_2 as well as changing the splitting pattern [3–7]. Our results illustrate that Fe, Cu and Mn partially oxidized the L-Cys –SH group and create cystine at low pH levels. CH_2 group of cystine moved to lower field (4.1 ppm) compared to that of L-Cys (3.8 ppm) because formation of a thiol bond between two L-Cys deshields the electron layer of neighboring carbon nucleus.

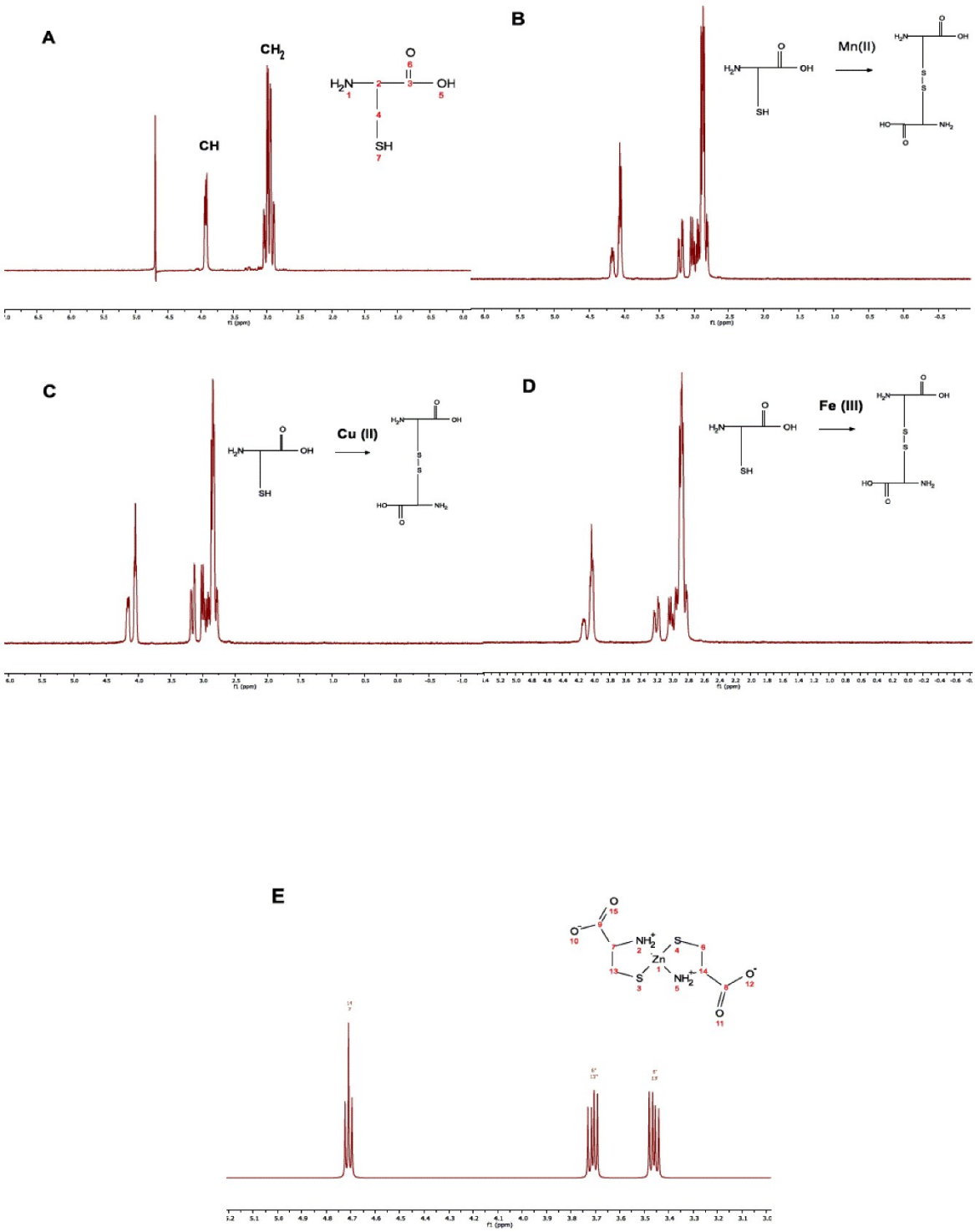

Figure 1S ^{1}H NMR spectra obtained from pure L-Cys (A), Mn(II)/L-Cys (B), Cu(II)/L-Cys (C), Fe(III)/L-Cys (D) and $Zn(Cys)_2$ complex (E) diluted in D_2O at a pH level of 3.

Kinetic experiment: Michaelis Menten reaction proceed by recording the velocity of chlorination of thionin (8-50 μM) and NR (10-70 μM) in various concentrations. To obtain the kinetic parameters of chlorination reaction, lineweaver Burk plot drew based on Michaelis Menten, and kinetic parameters obtained using Eq. 1. Turn over numbers obtained from biocatalysts demonstrate that CPO is a high performing enzyme compared with mettalo micelle but the specific activity of micellar artificial enzyme is comparable with that of native one. Our results indicate that Zn complex revives 10% of native enzyme's activity (Table 1S).

Table 1S Kinetic parameters of native and artificial catalysts. Concentrations of CPO and artificial metallo-micelle in all cases were 5 nM and 20 μM (Zn^{2+}), respectively.

Catalyst	K_m	V_m	$k_{cat}(V_m/E_t)$	***Specific Activity (units/ml)***
Native *Chloroperoxidase* (CPO)	0.06	0.12	36	420[1]
Metallo-micelle using Zn center	0.055	0.043	0.0039	-

Differentiate scanning Calorimetry (DSC): Thermal titration decomposed the tree dimensional structure of biomolecules and denature the spatial orientation of molecules. DSC experiment provides a thermal diagram from structural deformation of molecule by titration of the temperature. Obtained results show that denaturation of DTAB micelle occurs at 32.8 °C (Scheme 1S, Top and fig. 2S). Participation of SDS surfactants within DTAB micelle increases its thermal stability. In fact. Insertion of SDS not only contributes in hydrophobic forces but also decreases the repulsion between cationic charged head DTAB and forms electrostatic interactions at the surface of micelle (Scheme 1, Below).

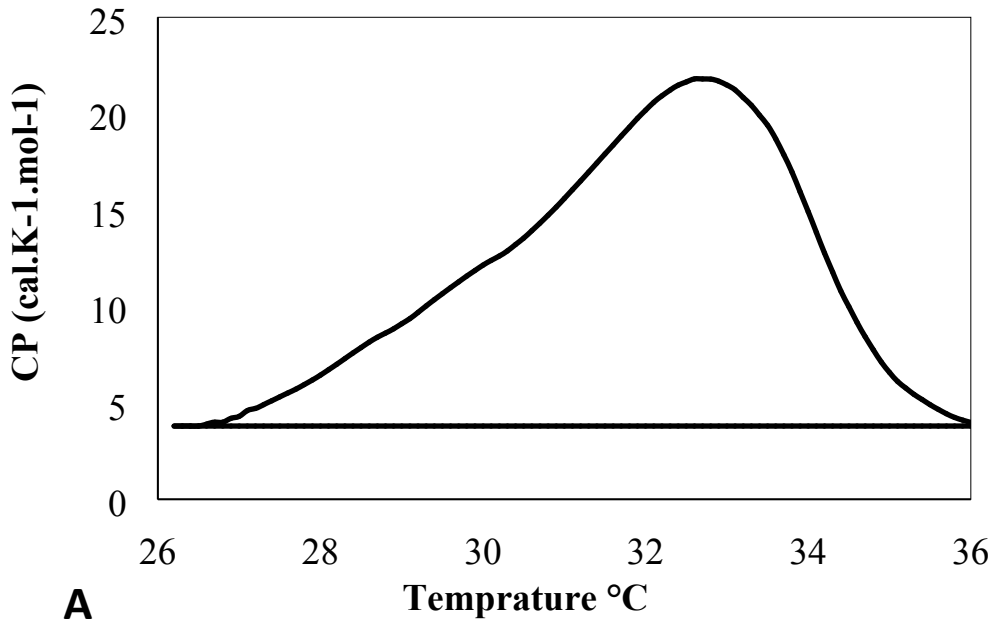

A

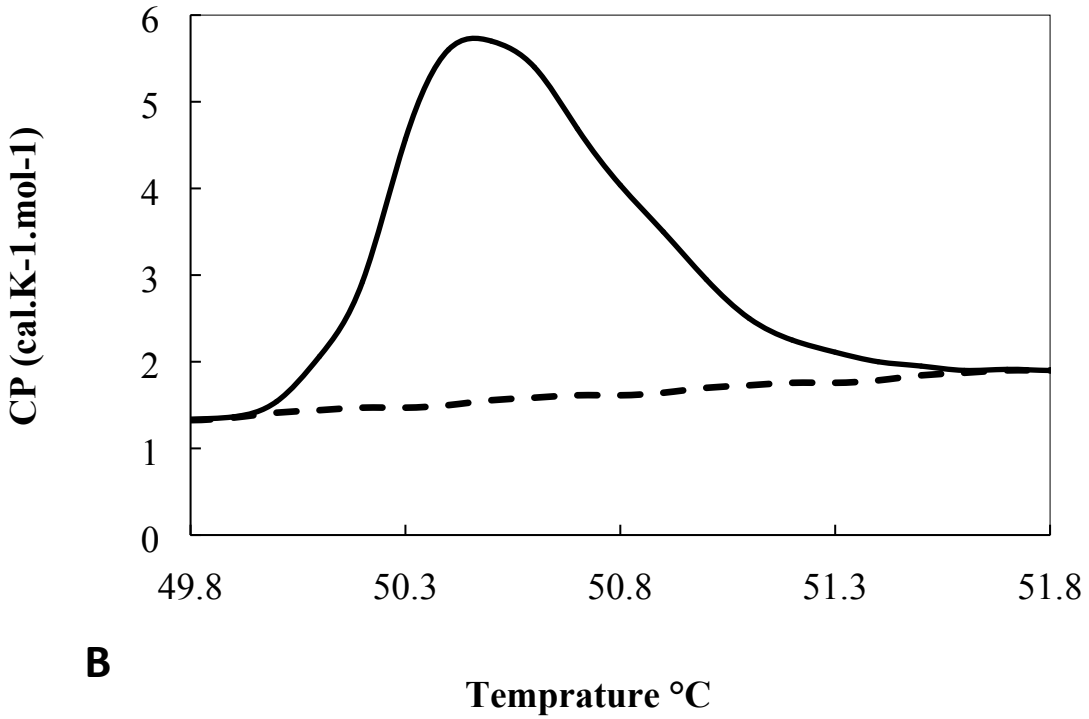

Figure 2S Calorimetric plot obtained from DTAB (A) and SDS/DTAB (B) micellar solutions.

Table 2S Calorimetric Parameters obtained from the Fitted Curves.

Thermodynamic parameters	**T_m**	**ΔH(kcal/mol)**	**ΔS(kcal/K. mol)**
Mixed Micelle (A)	32.8	75.6	0.25
Metallo-micelle (B)	50.4	0.1	0.00

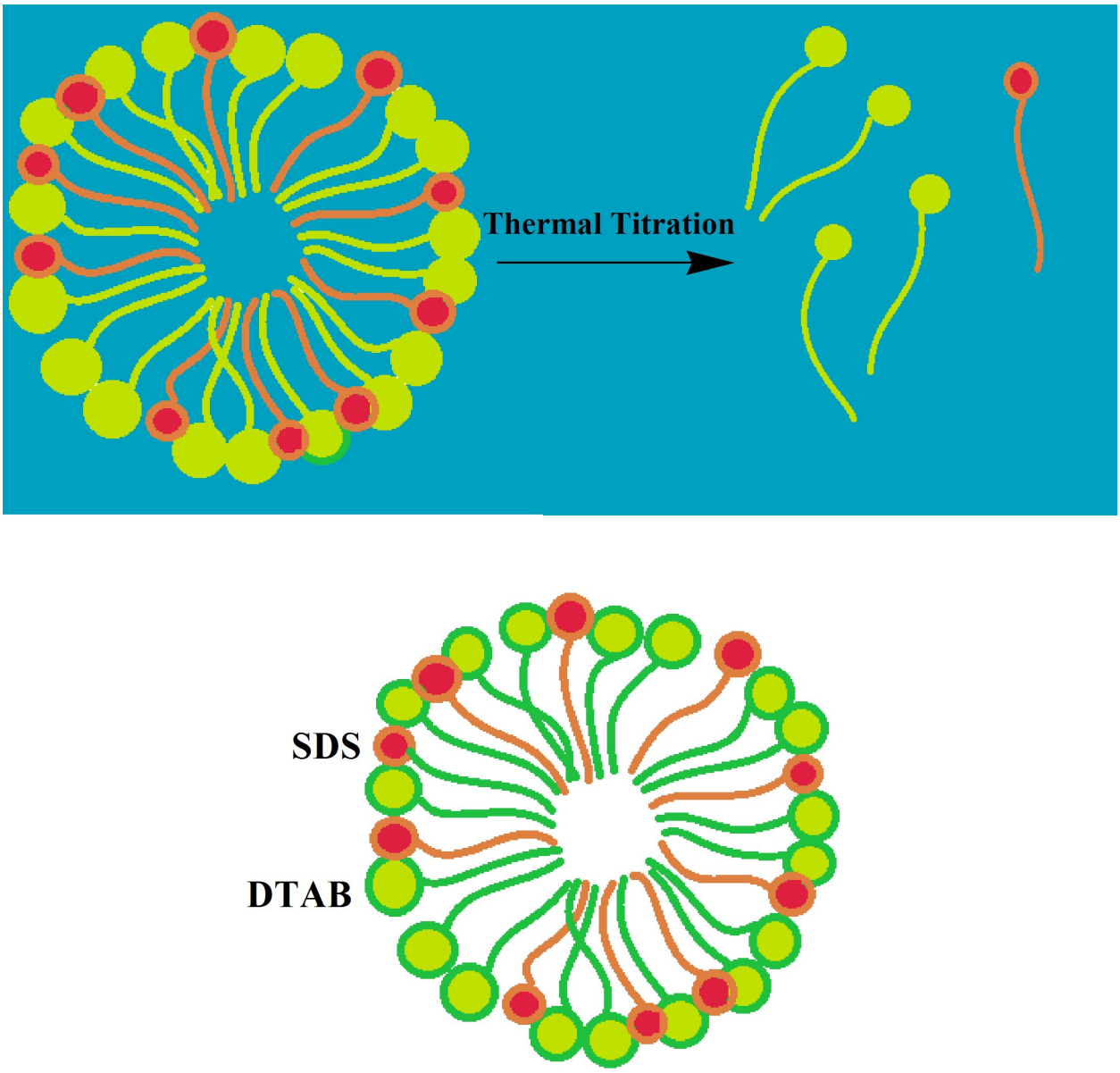

Scheme 1S Top: schematic images of micelle denaturation. Below: SDS/DTAB forms mixed micelle at low pH levels.

Isothermal Titration Calorimetry (ITC): Isothermal Titration Calorimetry (ITC) illustrates the insertion of one $Zn(Cys)_2$ complex within each micelle, and the insertion occurred trough a exothermic enthalpy driven reaction (Fig. S3 and table S3).

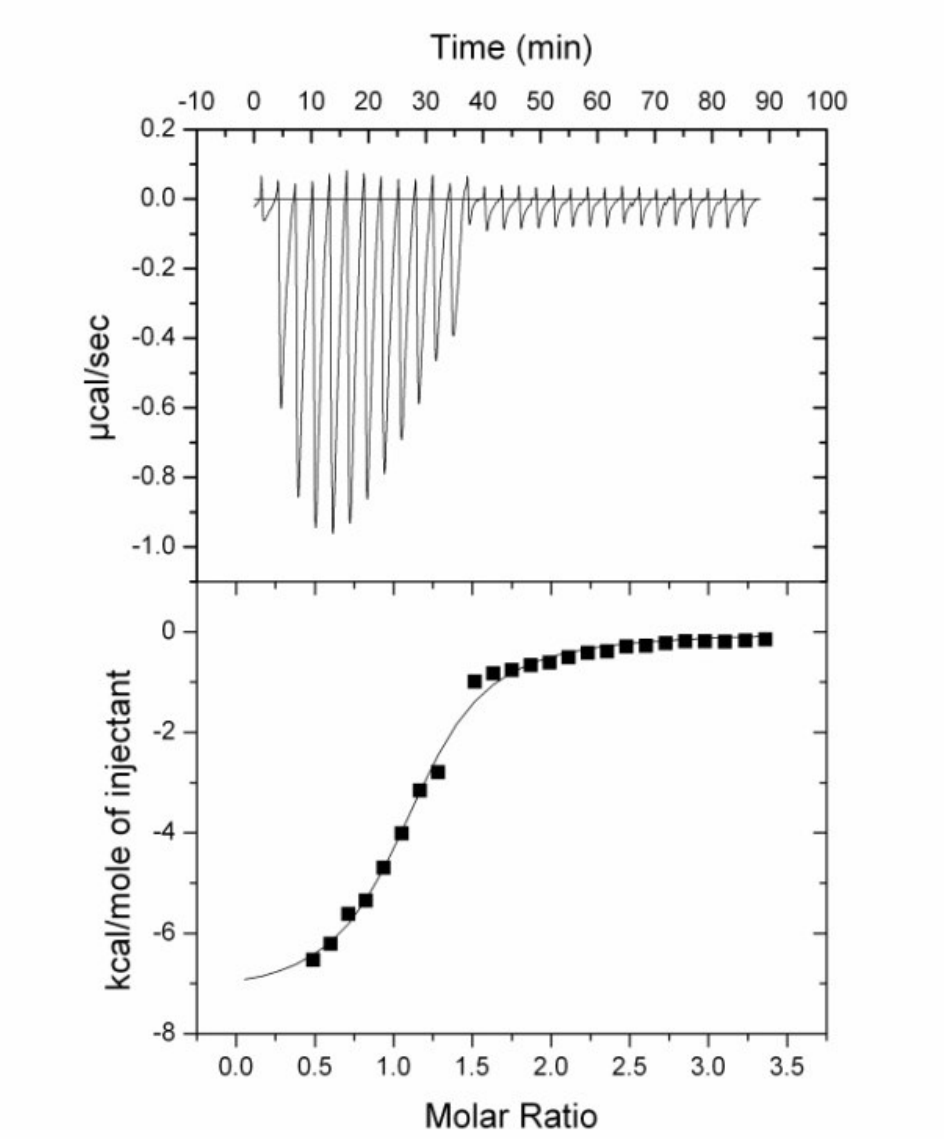

Figure 3S TEM images obtained from pure micellar CTAB (Top) and Zn(II)/L-Cys in micellar CTAB (Below) at a pH level of 3.

Table 3S Thermodynamic parameters obtained from ITC.

Reaction	N	K_a	ΔH (kJ/mol)	ΔG (kJ/mol)	ΔS (kJ/mol.K)
Addition of Cys to Zn^{2+} solution at pH 3	1.11	1.71×10^5	-30.514	-31.184	-0.002

Transition Electron Microscopy (TEM): To have a better understanding form micellar scaffold obtained from various mixtures, TEM images were recorded. Micelles constructed from pure SDS at low pH values indicates aggregate formation but DTAB scaffold are solubilized as curve-like micelles (Fig. 4S, A). Low pH decreases the repulsion forces between anionic charged head of SDS and leads toward aggregation which is in a good agreement with previous report (Fig. 4S, B) [8]. Aqueous mixture of SDS/DTAB forms a stable and homogeny micellar solution (Fig. 4S, C and D).

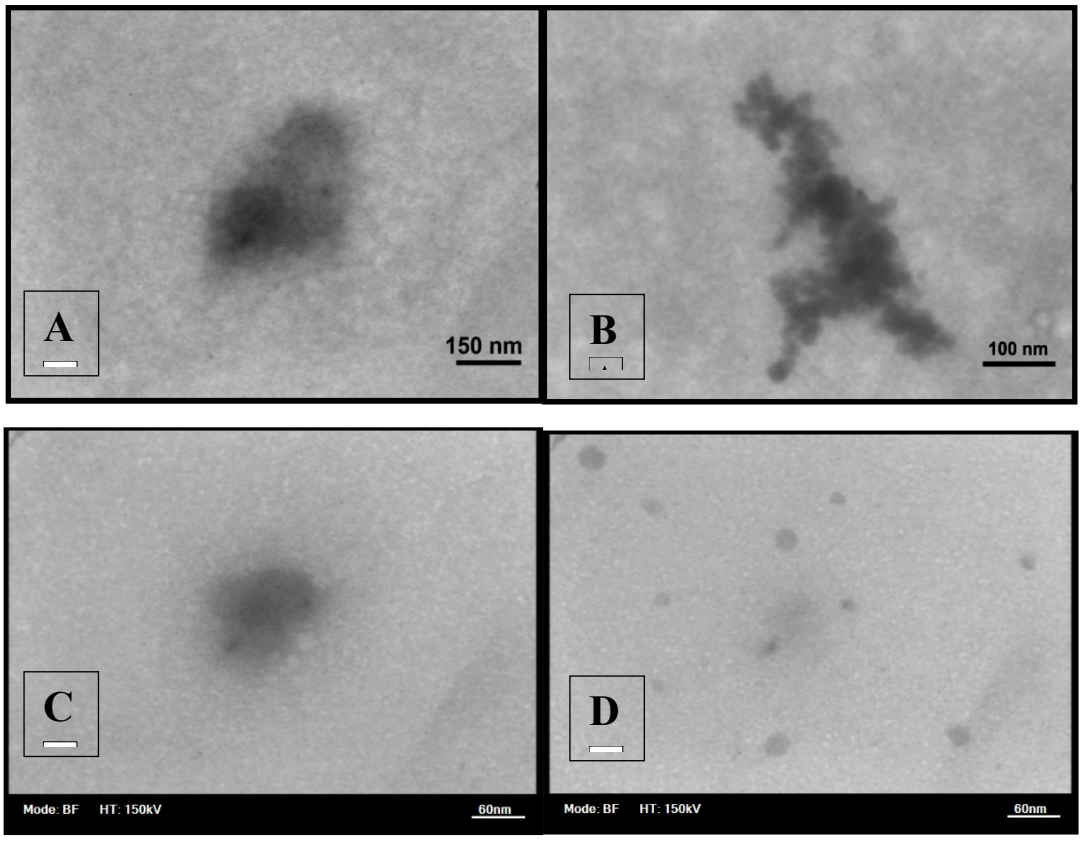

Figure 4S TEM images obtained from DTAB (A), SDS (B), SDS/SDAT (C and D) micellar solutions.

Dynamic Light Scattering (DLS): Next, dynamic radius of micellar structure was measured using DLS analysis. According to table 4S, SDS creates a 1.4 μm aggregate, while DTAB forms a 20 nm particles. Addition of SDS to a solution DTAB contributes in formation of 58 nm micelle formation. Based on these data, it concludes that SDS/DTAB forms an appropriate structure in wide ranges of pH values. Measuring the diameter of SDS/DTAB micelle in different pH values indicates that incearing of pH levels contributes in aggregate formation, whereas decrease of pH values accompanying in decomposition of micelles (Fig. 5S).

Table 4S DLS parameter obtained from DTAB and $Zn(Cys)_2$ DTAB micelles.

Compounds	Diameter, nm	Zeta potential, mV
DTAB, 25 mM	20	+30
SDS, 25 mM	1400	-120
DTAB /SDS, 25 mM,5 mM,	58	+15
DTAB /SDS, 25 mM,5 mM, $Zn(Cys)_2$, (0.1 mM $ZnCl_2$ + 1.2 mM L-Cys)	60	+14

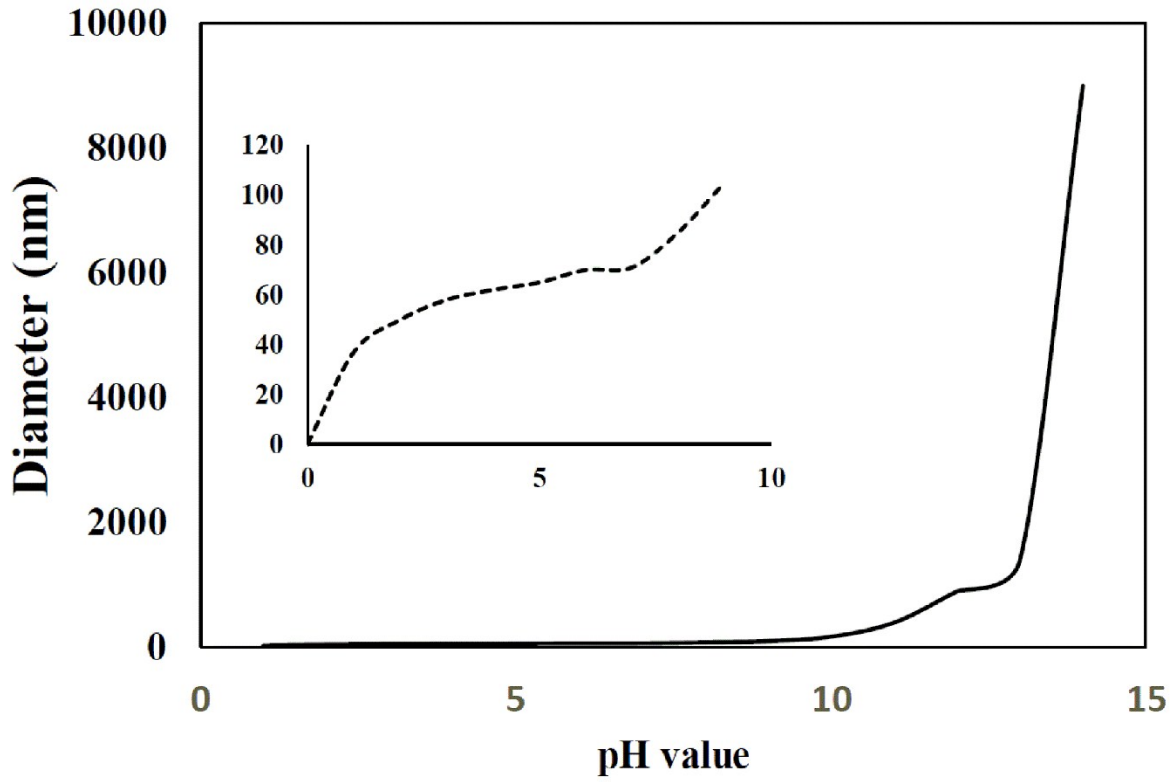

Figure 5S dynamic radii of SDS/DTAB micelle in different pH values. Inset shows the changes of micelle's diameter in 0-10 pH values ranges.

In conclusion, micellar characterization introduced a water soluble scaffold which resist high temperatures and is capable of applying in wide ranges of pH values compared to the native CPO. Using two types of surfactant involving cationic and anionic monomers provides a micellar scaffold with astonishing features such as thermal and pH resistance, and it open a new window toward the scaffold engineering.

References

1 K. M. Manoj and L. P. Hager, *Anal. Biochem.*, 2006, **348**, 84–86.
2 D. Zhang, Z. Chen, H. Omar, L. Deng and N. M. Khashab, *ACS Appl. Mater. & Interfaces*, 2015.
3 R. H. White, *J Label Compd Radiopharm*, 1987, **24**, 323–330.
4 A. R. Katritzky, N. G. Akhmedov and O. V. Denisko, *Magn. Reson. Chem.*, 2002, **41**,

37–41.
5 K. M. Dokken, J. G. Parsons, J. McClure and J. L. Gardea-Torresdey, *Inorganica Chim. Acta*, 2009, **362**.
6 A. G. Brolo, P. Germain and G. Hager, *J. Phys. Chem. B*, 2002, **106**, 5982–5987.
7 A. Pawlukojć, J. Leciejewicz, A. J. Ramirez-Cuesta and J. Nowicka-Scheibe, *Spectrochim. acta. Part Mol. Biomol. Spectrosc.*, 2005, **61**, 2474–2481.
8 Y. Zuev, D. Faizullin, B. Idiyatullin, F. Mukhitova, J.-M. Chobert, V. Fedotov and T. Haertl, *Colloid & Polym. Sci.*, 2004, **282**, 264–269.